Journal of Molecular Cell Biology (2026), 18, mjag016 https://doi.org/10.1093/jmcb/mjag016
Published online May 8, 2026

Article

ITIH5 drives adipocyte differentiation and obesity-associated metabolic dysregulation via PI3K/AKT signaling activation

Dan Li[1], Maoxiang Xu[1], Jie Li[1], Mengliu Yang[2], Gangyi Yang[2], and Ling Li[1,*]

[1] Key Laboratory of Medical Diagnostics of Ministry of Education, Department of Laboratory Medicine, Chongqing Medical University, Chongqing 400016, China
[2] Department of Endocrinology, the Second Affiliated Hospital, Chongqing Medical University, Chongqing 400010, China
* Correspondence to: Ling Li, E-mail: liling@cqmu.edu.cn

Edited by Feng Liu

Obesity markedly increases the risk of type 2 diabetes, highlighting the urgent need for novel therapeutic targets. The inter-alpha-trypsin inhibitor heavy chain 5 (ITIH5), which is predominantly produced by the adipose tissue, has emerged as a potential regulatory factor in obesity; however, the specific underlying mechanisms remain unclear. In this study, we identified ITIH5 as a key factor upregulated in obesity and closely associated with adipocyte differentiation and metabolic regulation. ITIH5 expression was significantly elevated in the adipose tissue of obese mice. *In vitro* experiments revealed that ITIH5 knockdown suppressed 3T3-L1 adipocyte differentiation, lipid accumulation, and inflammatory cytokine secretion, whereas ITIH5 overexpression markedly enhanced these effects. Mechanistically, activation of the PI3K/AKT signaling pathway was found to mediate ITIH5-induced adipogenic differentiation and lipid synthesis. Consistent with these findings, *in vivo* knockdown of ITIH5 in the inguinal white adipose tissue alleviated high-fat diet-induced obesity, reduced adipocyte hypertrophy, improved glucose tolerance, and increased energy expenditure. Conversely, overexpression of ITIH5 aggravated metabolic dysfunction. Collectively, these findings indicate that ITIH5 promotes adipogenesis and obesity progression via the PI3K/AKT pathway, providing a potential therapeutic target for obesity intervention.

Keywords: ITIH5, lipid metabolism, PI3K/AKT signaling, obesity

Introduction

Obesity is believed to be caused by excessive expansion of the white adipose tissue (WAT) due to increased adipocyte hypertrophy and the differentiation of adipocyte precursors into mature adipocytes (Blüher, 2019; Khaliq et al., 2025). The adipose tissue was initially considered a form of connective tissue and an energy storage organ *in vivo*. In recent years, the adipose tissue has also been recognized as an important endocrine organ, which can release various bioactive factors, including hormones, cytokines, extracellular matrix (ECM) proteins, and growth and vascular active factors. These cytokines are released into the circulation and act on different tissues and organs, regulating feeding behavior, inflammation and immune responses, glucose and lipid metabolism, etc. (Bruder and Bruder-Nascimento, 2025; Lin and Jensen, 2025).

The inter-alpha inhibitor heavy chain (ITIH) family consists of secreted glycoproteins that play a significant role in regulating the ECM and modulating inflammation (Anveden et al., 2012). ITIH1–ITIH4 are mainly expressed in the liver, where they form an inter-alpha-trypsin inhibitor complex with a bikunin light chain, which functions as a protease inhibitor (Chan et al., 1995; Zhuo et al., 2004). Under the mediation of bikunin, ITIHs are capable of binding to hyaluronic acid and play a role in stabilizing the ECM (Hutadilok et al., 1988; Hamm et al., 2008; Chen et al., 2016). Recent studies have shown that in type 2 diabetes (T2D) patients with poor blood

Received November 23, 2025. Revised February 27, 2026. Accepted March 15, 2026.
© The Author(s) (2026). Published by Oxford University Press on behalf of *Journal of Molecular Cell Biology*, CEMCS, CAS.
This is an Open Access article distributed under the terms of the Creative Commons Attribution-NonCommercial License (https://creativecommons.org/licenses/by-nc/4.0/), which permits non-commercial re-use, distribution, and reproduction in any medium, provided the original work is properly cited. For commercial re-use, please contact reprints@oup.com for reprints and translation rights for reprints. All other permissions can be obtained through our RightsLink service via the Permissions link on the article page on our site-for further information please contact journals.permissions@oup.com

glucose control, circulating levels of ITIH1 and ITIH4 are notably elevated, with a decrease following successful blood glucose management (Tvarijonaviciute et al., 2016; Gourgari et al., 2019; Kim et al., 2019). Animal studies have shown that circulating levels of ITIH3 increase in obese rats and negatively correlate with body weight (Choi et al., 2012). These studies suggest that the ITIH family is associated with obesity and metabolic disorders.

ITIH5 is a 105-kDa secreted protein, the fifth member of the ITIH family. ITIH5 is primarily expressed in the placenta and adipose tissue (Anveden et al., 2012), indicating its potential involvement in metabolic processes *in vivo* (Desoye and Hauguel-de Mouzon, 2007; Bond et al., 2022). Clinical studies have shown that ITIH5 expression is significantly elevated in adipose tissues from obese patients and decreases with body weight loss during a low-calorie diet. Additionally, the expression of ITIH5 correlates significantly with body mass index, blood pressure, blood lipids, glucose metabolism indicators, and C-reactive protein levels. Furthermore, the expression pattern of ITIH5 resembles that of classical adipokines, such as leptin and inhibin-β. Therefore, it is hypothesized that ITIH5 may function as a novel adipokine (Desoye and Hauguel-de Mouzon, 2007; Anveden et al., 2012). Here, we investigated the role of ITIH5 in adipocyte differentiation and its impact on the metabolic phenotype of diet-induced obese mice, as well as its possible molecular mechanisms.

Results

ITIH5 expression is upregulated in the adipose tissue of obese mice and mature adipocytes

To investigate the expression pattern of ITIH5 in mice, we initially assessed the transcription level of ITIH5 in various tissues of adult wild-type (WT) mice. As depicted in Figure 1A, quantitative real-time polymerase chain reaction (qRT-PCR) revealed the highest *Itih5* mRNA expression level in the adipose tissue, followed by the stomach and small intestine. Furthermore, immunohistochemistry (IHC) staining demonstrated that ITIH5 was mainly localized in the cytoplasm of adipocytes and markedly upregulated in the adipose tissue of mice fed a high-fat diet (HFD) (Figure 1B). Data analysis based on a public database (GSE123394) showed that *Itih5* mRNA expression significantly increased in the adipose tissue of mice fed a HFD compared to those fed a low-fat diet (LFD) (Figure 1C, left panel). Additionally, analysis of published data (GSE8505) indicated that *Itih5* expression level was higher in mature adipocytes than in stromal vascular fractions (SVFs) (Figure 1C, right panel). To further investigate the relationship between ITIH5 and obesity, we examined the mRNA and protein levels of ITIH5 in the epididymal WAT (eWAT) and inguinal WAT (iWAT) of HFD-fed WT mice, ob/ob mice, and db/db mice. The results showed that ITIH5 expression levels were significantly upregulated in the adipose tissues of these three obese mouse models (Figure 1D; Supplementary Figure S1A and B). The analysis of a publicly available single-cell mouse database (Tabula Muris) revealed that *Itih5* gene expression was most abundant in mesenchymal stem cells within the adipose tissue (Figure 1E). Similarly, the analysis of a public dataset (GSE198482) revealed that the transcription level of ITIH5 was significantly higher in the adipose progenitor cells with adipogenic induction compared to non-induced cells (Figure 1F). To understand the impact of adipocyte differentiation on ITIH5 expression, we examined ITIH5 expression changes during the differentiation of 3T3-L1 cells and mouse primary adipocytes (MPA). Lipid contents significantly increased on Day 6, Day 9, and Day 12 of 3T3-L1 cell differentiation, as well as on Day 4, Day 6, and Day 8 of MPA differentiation (Figure 1G and H). The mRNA and protein expression levels of ITIH5 also significantly increased from Day 3 of 3T3-L1 cell differentiation and Day 4 of MPA differentiation, peaking on Day 12 and Day 8, respectively (Figure 1I and J). In addition, we observed a time-dependent increase in the secreted ITIH5 protein levels, suggesting that ITIH5 is actively secreted during adipocyte differentiation (Supplementary Figure S1C).

ITIH5 knockdown inhibits 3T3-L1 cell differentiation, lipid accumulation, and adipokine secretion

To investigate whether ITIH5 has a regulatory role in adipocyte differentiation *in vitro*, 3T3-L1 cells were transfected with Ad-shITIH5 to knock down ITIH5. As expected, both mRNA and protein levels of ITIH5 were significantly reduced, with Ad-shITIH5-3 showing the most significant effect (Figure 2A). ITIH5 knockdown notably inhibited 3T3-L1 cell differentiation and lipid accumulation (Figure 2B and C), as well as the protein expression of genes related to adipose differentiation (PPARγ, C/EBPα, and FABP4) and lipogenesis (SREBP1c, FAS, SCD1, and CD36) (Figure 2D). Secretion of inflammatory factor by adipocytes is essential for the progression of obesity and associated metabolic disorders (Bruder and Bruder-Nascimento, 2025). We found that both *Il-6* mRNA expression in cell lysates and secreted IL-6 level in culture supernatants as determined by enzyme-linked immunosorbent assay (ELISA) significantly decreased following ITIH5 knockdown (Figure 2E). Given that ITIH5 is involved in regulating the ECM (Wu et al., 2025), we further investigated the effects of ITIH5 knockdown on ECM homeostasis. The results demonstrated that ITIH5 silencing markedly suppressed Collagen I, Collagen III, and TIMP1 protein expression, while promoting MMP9 expression (Supplementary Figure S2A).

ITIH5 overexpression promotes 3T3-L1 cell differentiation, lipid accumulation, and adipokine secretion

Next, 3T3-L1 cells were transfected with Ad-ITIH5 to overexpress ITIH5 at both mRNA and protein levels (Figure 3A). ITIH5 overexpression notably promoted 3T3-L1 cell differentiation and lipid accumulation (Figure 3B and C), as well as the protein levels of PPARγ, C/EBPα, FABP4, SREBP1c, FAS, SCD1, and

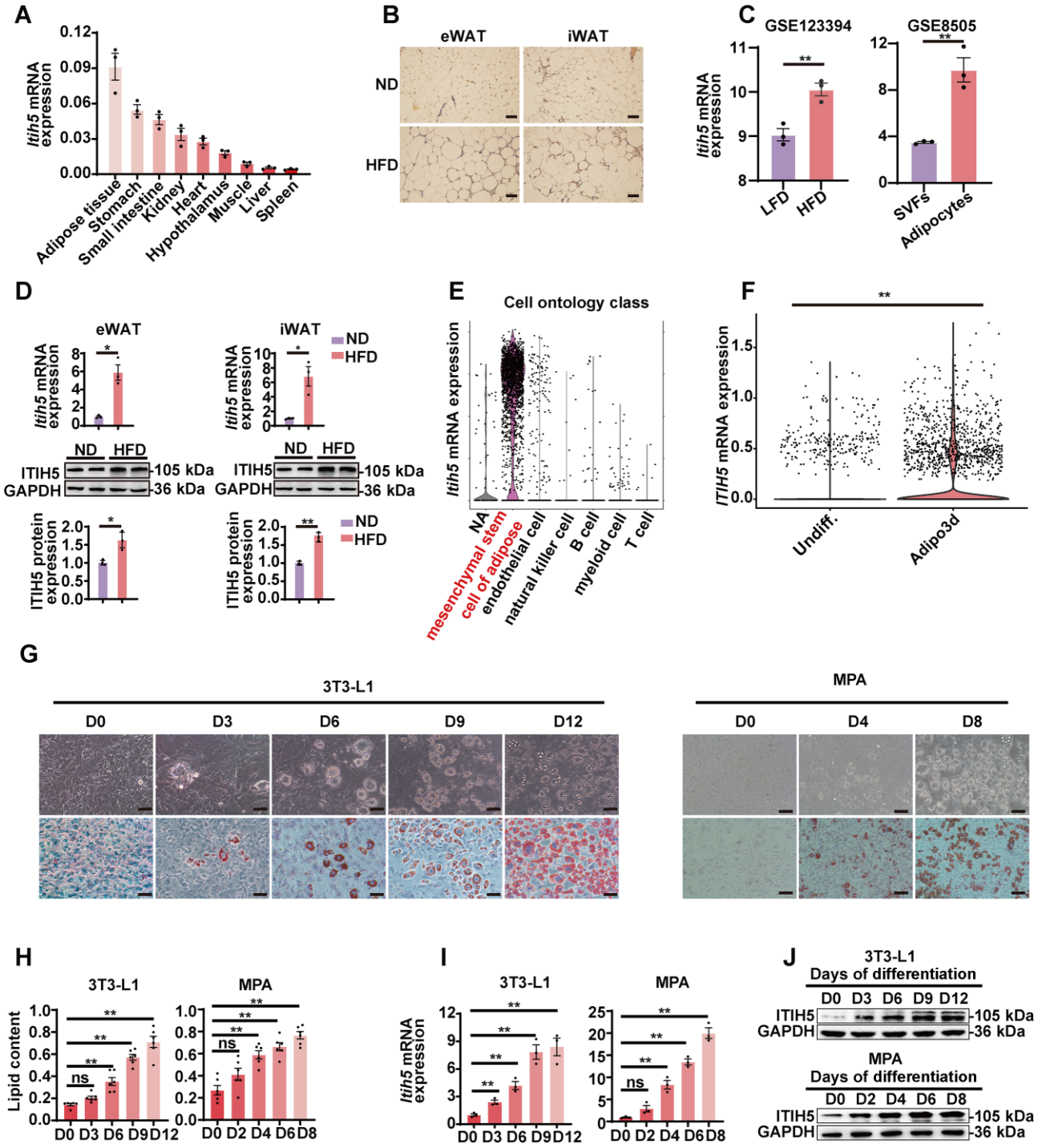


Figure 1 ITIH5 expression during adipocyte differentiation and in the adipose tissue of mice. (**A**) The tissue distribution of *Itih5* mRNA expression in WT mice. (**B**) IHC staining for ITIH5 in adipose tissues of ND- and HFD-fed WT mice (scale bar, 50 μm). (**C**) *Itih5* mRNA expression in adipose tissues of LFD- and HFD-fed WT mice (GSE123394; left panel) and in the isolated SVFs and adipocytes (GSE8505; right panel). (**D**) The mRNA and protein expression of ITIH5 in adipose tissues of ND- and HFD-fed C57BL/6 J (WT) mice. Total protein loading: 30 μg. (**E**) *Itih5* mRNA expression in the adipose tissue of mice (https://tabula-muris.sf.czbiohub.org/). (**F**) *Itih5* mRNA in human adipose tissue-derived mesenchymal progenitor cells treated with (Adipo3d) or without (undiff.) adipogenic induction (GSE198482). (**G** and **H**) Oil-Red-O staining (**G**, scale bar, 20 μm) and lipid contents in culture medium (**H**) from 3T3-L1 cells (left panel) and MPA (right panel). (**I** and **J**) The mRNA (**I**) and protein (**J**) expression of ITIH5 during adipocyte differentiation. Total protein loading: 30 μg. Data are shown as mean ± SEM ($n = 3$ or 4 mice for each group or ≥3 independent experiments). ns, no significance; *$P < 0.05$, **$P < 0.01$.

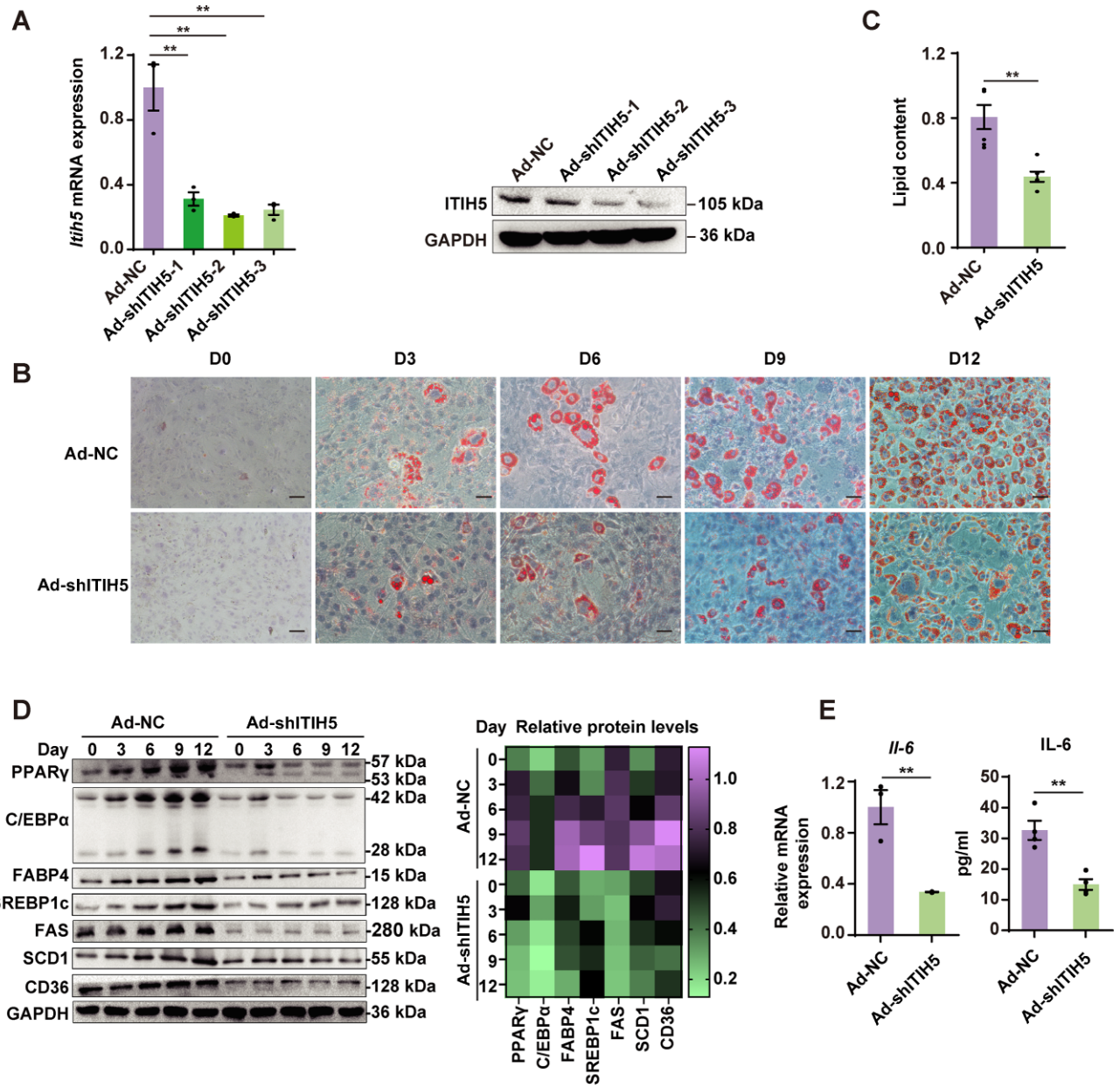


Figure 2 ITIH5 knockdown inhibits lipid accumulation in 3T3-L1 adipocytes. (**A**) The mRNA and protein expression of ITIH5 in 3T3-L1 cells transfected with Ad-shITIH5-1–3 or Ad-NC. Total protein loading: 30 μg. (**B**) Oil-Red-O staining for lipid content during 3T3-L1 adipocyte differentiation (scale bar, 20 μm). (**C**) Lipid contents in 3T3-L1 cells transfected with Ad-shITIH5-3 or Ad-NC. (**D**) The protein expression of genes related to lipid metabolism during 3T3-L1 adipocyte differentiation. Total protein loading: 30 μg. (**E**) *Il-6* mRNA expression levels in 3T3-L1 cells (left panel) and secreted IL-6 protein levels in culture medium (right panel). Data are shown as mean ± SEM ($n \geq 3$ independent experiments). $^{**}P < 0.01$.

CD36 (Figure 3D). Both *Il-6* mRNA expression in cell lysates and secreted IL-6 level in culture supernatants significantly increased following ITIH5 overexpression (Figure 3E). Furthermore, ITIH5 overexpression markedly promoted Collagen I, Collagen III, and TIMP1 protein expression, while suppressing MMP9 expression (Supplementary Figure S2B), revealing a shift in the ECM remodeling balance toward matrix accumulation.

ITIH5 knockdown in the iWAT ameliorates HFD-induced obesity

To investigate the role of ITIH5 in regulating obesity and metabolic phenotypes *in vivo*, 8-week-old WT mice were fed either a normal chow diet (ND) or a HFD for 12 weeks and then (20-week-old) injected *in situ* with Ad-shITIH5 or Ad-NC in the iWAT (Figure 4A). Seven days after the initial injection, ITIH5 protein expression was remarkably reduced in the iWAT of the

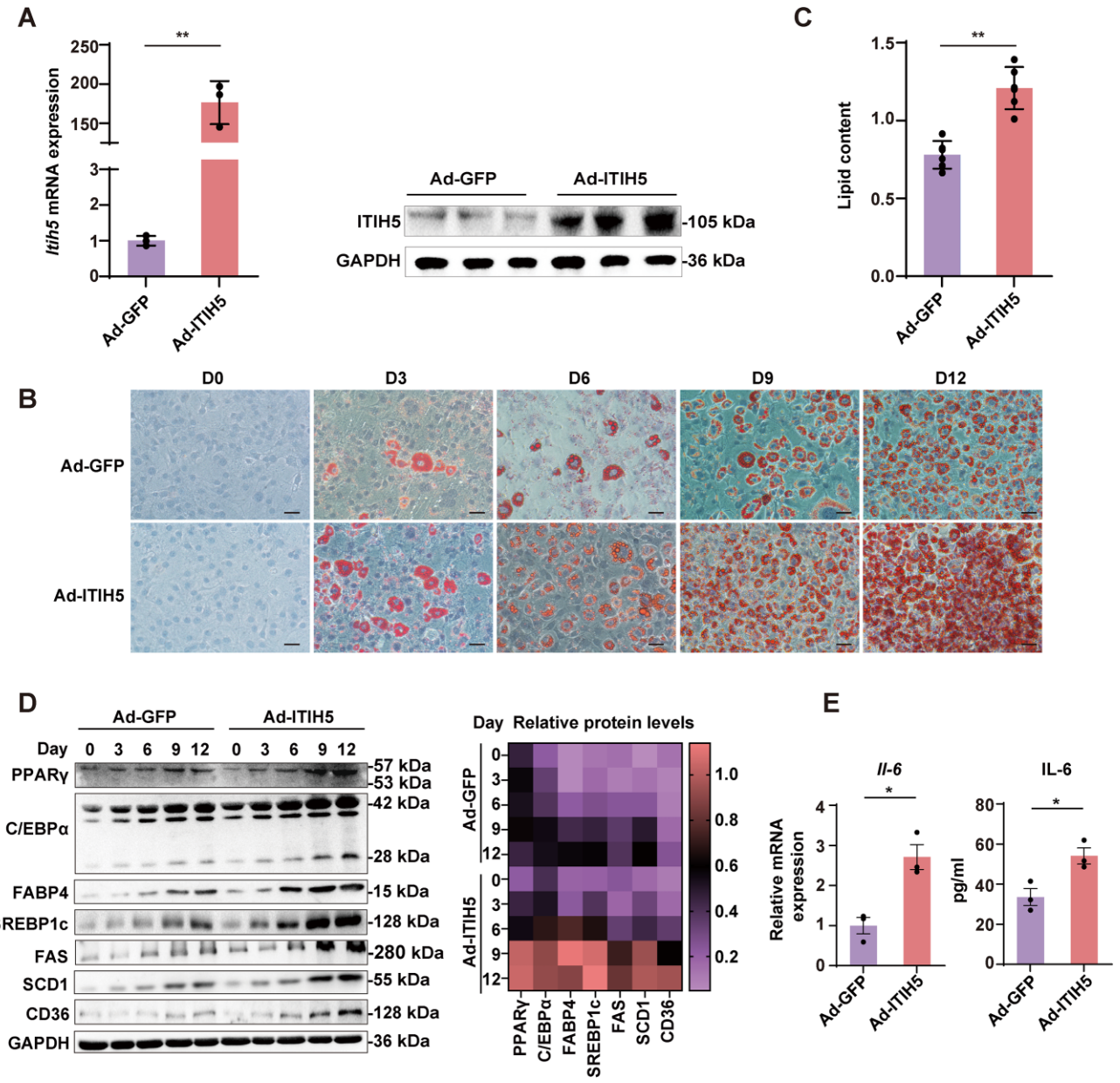


Figure 3 ITIH5 overexpression promotes lipid accumulation in 3T3-L1 adipocytes. (**A**) The mRNA and protein expression of ITIH5 in 3T3-L1 cells transfected with Ad-ITIH5 or Ad-GFP. Total protein loading: 30 μg. (**B**) Oil-Red-O staining for lipid content during 3T3-L1 adipocyte differentiation (scale bar, 20 μm). (**C**) Lipid contents in 3T3-L1 cells transfected with Ad-ITIH5 or Ad-GFP. (**D**) The protein expression of genes related to lipid metabolism during 3T3-L1 adipocyte differentiation. Total protein loading: 30 μg. (**E**) *Il-6* mRNA expression levels in 3T3-L1 cells (left panel) and secreted IL-6 protein levels in culture medium (right panel). Data are shown as mean ± SEM ($n \geq 3$ independent experiments). *$P < 0.05$, **$P < 0.01$.

Ad-shITIH5 group (Figure 4A). ITIH5 knockdown did not result in phenotypic changes in ND-fed mice (Figure 4B–G). However, in HFD-fed mice, ITIH5 knockdown resulted in significantly lower body weight (Figure 4B and C), lower iWAT weight (Figure 4E and F), smaller adipocyte size (Figure 4G), and decreased ECM deposition as evidenced by Masson's trichrome and Sirius Red staining (Supplementary Figure S3C), while not affecting food intake (Figure 4D). Notably, there was no significant change in the expression levels of inflammatory factors between the Ad-shITIH5 and Ad-NC groups (Supplementary Figure S3A and B), indicating that adenovirus injection did not elicit a significant inflammatory response.

Changes in the adipose tissue are often associated with glucose and lipid metabolism (Santoro and Kahn, 2023). Glucose tolerance test (GTT) and insulin tolerance test (ITT) revealed that ITIH5 knockdown enhanced glucose tolerance

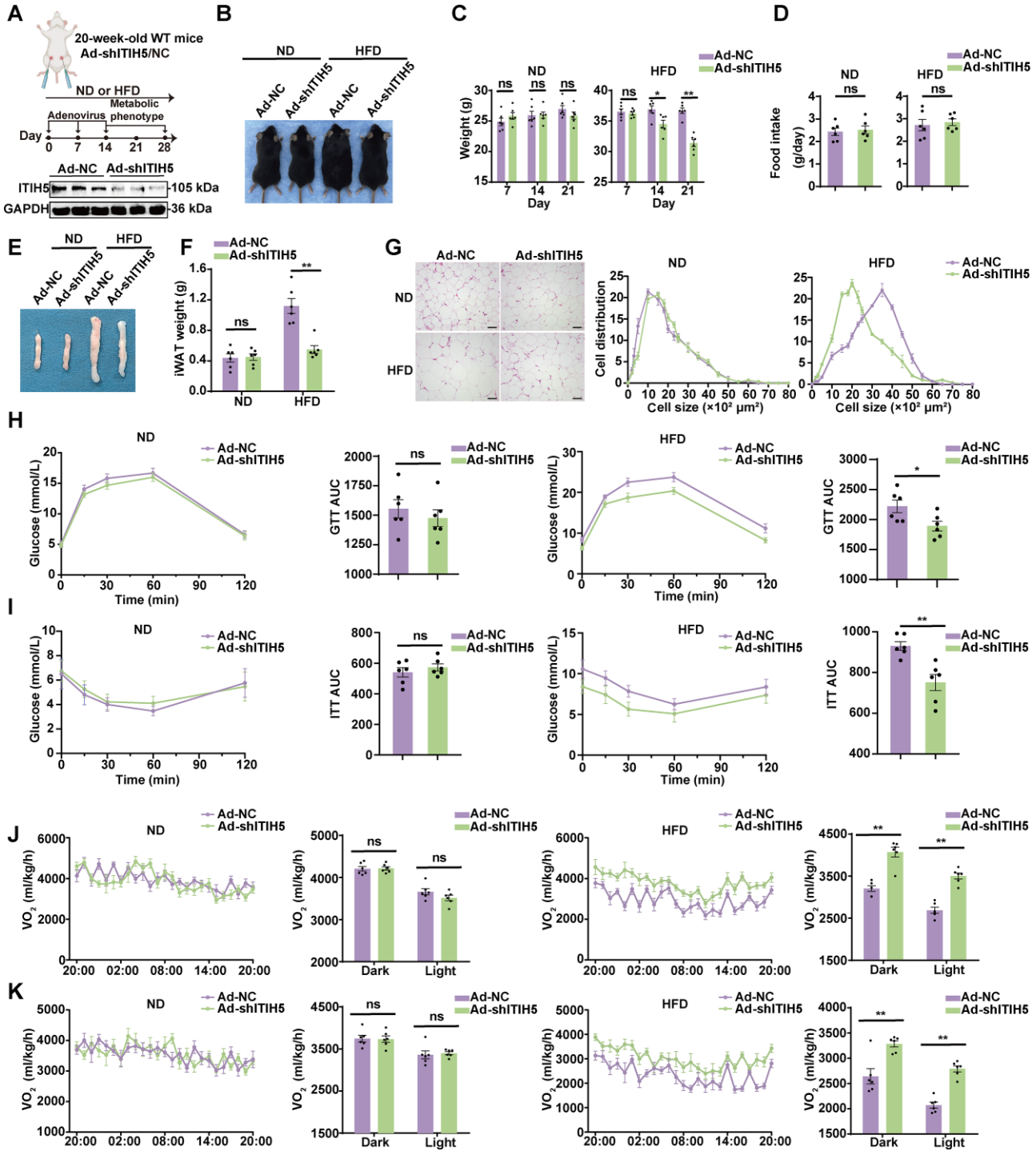


Figure 4 Knockdown of ITIH5 in the adipose tissue weakens HFD-induced obesity. (**A**) Experimental schematic diagram. ND- and HFD-fed male WT mice were subjected to Ad-shITIH5 or Ad-NC injection into bilateral iWAT as indicated. ITIH5 protein expression in the iWAT was detected on Day 7. (**B**) Representative image of ND- and HFD-fed male WT mice, 1 week after the third injection (Day 21). (**C**) Body weight on Days 7, 14, and 21 after the initial adenovirus injection. (**D**) Daily food intake. (**E** and **F**) Representative gross images (**E**) and weight (**F**) of mouse iWAT. (**G**) Representative H&E staining of the iWAT (scale bar, 50 μm) and quantification of adipocyte size in H&E sections. (**H**) GTT and AUC_{GTT}. (**I**) ITT and AUC_{ITT}. (**J**) The 24 h VO_2 and quantitative analysis. (**K**) The 24 h VCO_2 and quantitative analysis. AUC, area under glucose curve. Data are shown as mean ± SEM ($n = 6$ mice for each group or 3 independent experiments). ns, no significance; *$P < 0.05$, **$P < 0.01$ vs. Ad-NC.

and insulin responsiveness in HFD-fed mice but not in ND-fed mice (Figure 4H and I). We further assessed energy expenditure using metabolic cages and found that ITIH5 knockdown significantly increased oxygen consumption (VO_2) and carbon dioxide consumption (VCO_2) in HFD-fed mice but not in ND-fed mice (Figure 4J and K). Consistently, ITIH5 knockdown markedly increased both UCP1 protein expression and cAMP content in the iWAT of HFD-fed mice (Supplementary Figure S3D–F). These findings suggest that ITIH5 knockdown leads to increased energy expenditure and alleviates HFD-induced obesity.

ITIH5 overexpression in the iWAT exacerbates HFD-induced obesity

Next, we constructed a mouse model in which ITIH5 protein expression in the iWAT remarkably increased 7 days after the initial Ad-ITIH5 injection (Figure 5A) and the adenovirus injection did not cause changes in the levels of inflammatory markers (Supplementary Figure S4A and B). ITIH5 overexpression in the iWAT did not show significant effect on metabolic phenotypes in ND-fed mice (Figure 5B–I). However, in HFD-fed mice, ITIH5 overexpression resulted in significantly increased body weight (Figure 5B and C), iWAT weight (Figure 5E and F), adipocyte size (Figure 5G), and ECM deposition (Supplementary Figure S4C), while not affecting food intake (Figure 5D). Consistent with these metabolic alterations, ITIH5 overexpression markedly reduced both UCP1 protein expression and cAMP content in the iWAT of HFD-fed mice (Supplementary Figure S4D–F). Moreover, ITIH5 overexpression exacerbated glucose and insulin intolerance in HFD-fed mice but not in ND-fed mice (Figure 5H and I). Collectively, these results indicate that adipose-specific ITIH5 overexpression aggravates HFD-induced metabolic dysfunction.

PI3K/AKT signaling pathway is required for ITIH5 regulation of adipocyte metabolism

To elucidate the potential mechanisms underlying ITIH5 regulation of adipose differentiation and lipid accumulation, we performed RNA sequencing (RNA-seq) analysis with ITIH5-overexpressing 3T3-L1 cells. Principal component analysis (PCA) showed that Ad-ITIH5 and Ad-GFP samples were completely segregated (Figure 6A). A total of 680 differentially expressed genes (DEGs) were identified, including 475 downregulated genes and 205 upregulated genes (Figure 6B). Consistent with our cellular experiment results, genes related to adipogenesis (SCD1 and CD36) and adipocyte differentiation (PPARγ and C/EBPα) were significantly upregulated (Figure 6C). Gene set enrichment analysis (GSEA) further confirmed that ITIH5 overexpression positively regulated adipose differentiation (Figure 6D). Moreover, Kyoto Encyclopedia of Genes and Genomes (KEGG) pathway analysis revealed that the DEGs were significantly enriched in the PI3K–AKT signaling pathway (Figure 6E).

The PI3K/AKT signaling pathway is closely associated with adipocyte differentiation and glucose/lipid metabolism (Li et al., 2025; Liu et al., 2025; Wang et al., 2025). To examine whether ITIH5 functions through the PI3K/AKT pathway in adipocytes, SVFs were isolated from WT mice and differentiated into mature MPA, followed by Ad-ITIH5/GFP or Ad-shITIH5/NC transfection, respectively. Western blotting showed that ITIH5 overexpression significantly increased the phosphorylation levels of PI3K and AKT, while ITIH5 knockdown significantly inhibited PI3K/AKT phosphorylation (Figure 6F and G). Similar changes in PI3K/AKT phosphorylation levels were detected in the iWAT upon ITIH5 knockdown or overexpression (Supplementary Figures S3F and S4F). Additionally, treatment with a PI3K/AKT inhibitor (LY294002) reversed the stimulatory effect of ITIH5 overexpression on adipogenesis in MPA (Figure 6H–J). These results suggest that PI3K/AKT signaling is essential for ITIH5 to exert its metabolic regulatory effects on adipocytes.

Discussion

Obesity is a chronic metabolic disorder characterized by excessive fat accumulation, which is closely associated with T2D, cardiovascular disease, and various inflammatory conditions and poses a significant threat to global public health (Dai et al., 2025). While it is well-established that abnormal adipocyte differentiation is essential for the onset and progression of obesity, the specific molecular mechanisms remain incompletely understood. Therefore, it is crucial to investigate the regulatory mechanisms of adipocyte differentiation and lipid metabolism to develop new treatment strategies for obesity. In this study, through multilevel experimental evidence, we systematically elucidated the crucial role of ITIH5 in adipocyte differentiation and lipid metabolism. ITIH5 expression was significantly upregulated in adipose tissues from obese mice and during adipocyte differentiation, with secreted levels increasing in culture supernatants, confirming its secretion during adipogenesis. *In vitro* experiments demonstrated that ITIH5 knockdown inhibited adipocyte differentiation and lipid accumulation, while also reducing inflammatory cytokine levels. *In vivo*, ITIH5 knockdown alleviated diet-induced obesity, improved glucose tolerance and insulin sensitivity, and increased energy expenditure, whereas ITIH5 overexpression exacerbated obesity and metabolic disorders. Mechanistically, ITIH5 regulated adipocyte differentiation and lipid metabolism through the PI3K/AKT signaling pathway. Therefore, ITIH5 may serve as a potential target for obesity intervention.

ITIH5 is a member of the ITIH family and functions as a secreted ECM protein involved in maintaining ECM stability (Wu et al., 2025). In this study, we first investigated the expression pattern of ITIH5 and found that it was most highly expressed in adipose-derived mesenchymal stem cells, and its secretion gradually increased during adipocyte differentiation. These findings suggest that ITIH5 is induced during adipocyte differentiation and may regulate adipose tissue function through autocrine or paracrine mechanisms.

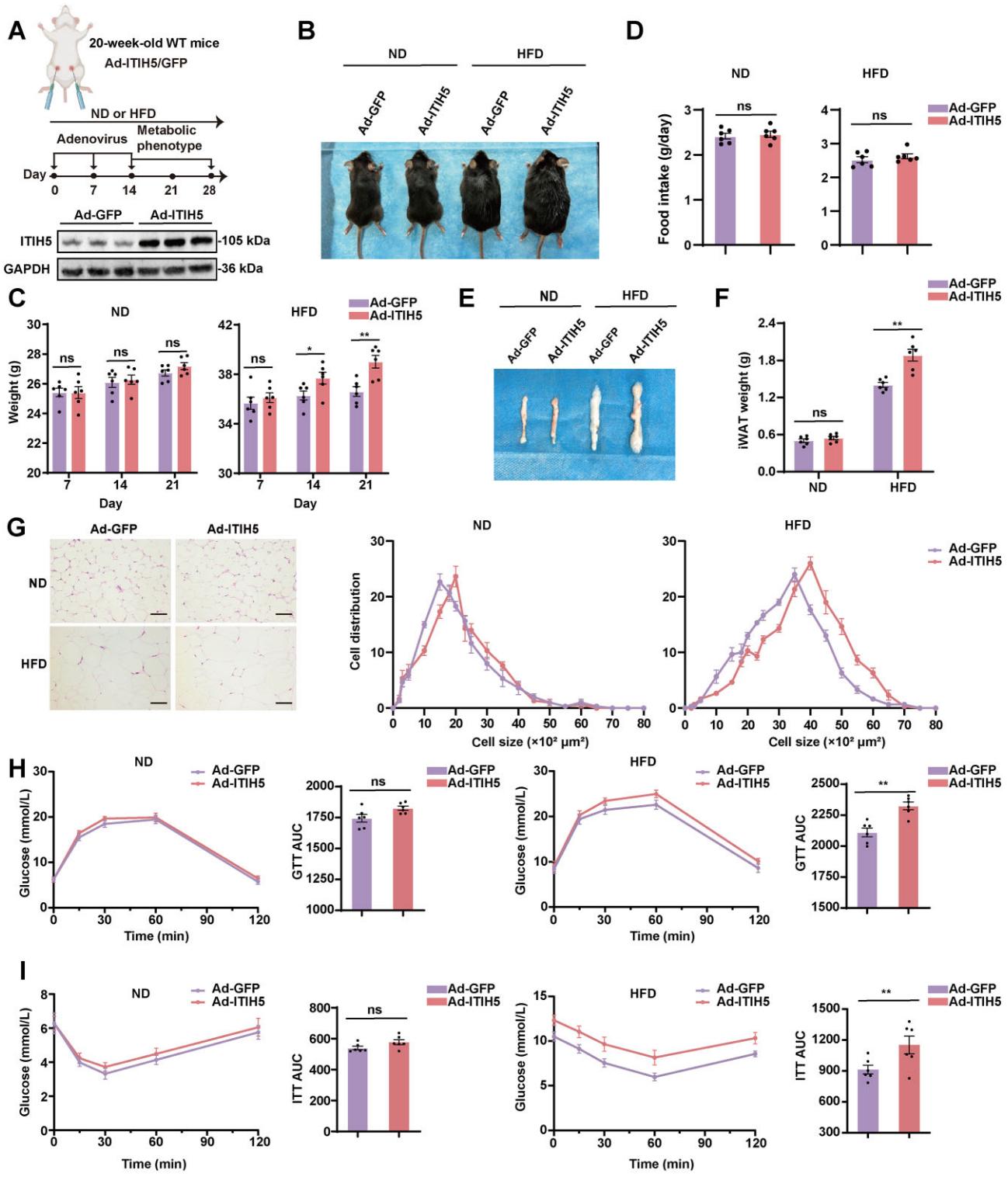


Figure 5 Overexpression of ITIH5 in the adipose tissue promotes HFD-induced obesity. (**A**) Experimental schematic diagram. ND- and HFD-fed male WT mice were subjected to Ad-ITIH5 or Ad-GFP injection into bilateral iWAT as indicated. ITIH5 protein expression in the iWAT was detected on Day 7. (**B**) Representative image of the mice on Day 21. (**C**) Body weight on Days 7, 14, and 21. (**D**) Daily food intake. (**E** and **F**) Representative gross images (**E**) and weight (**F**) of mouse iWAT. (**G**) Representative H&E staining of the iWAT (scale bar, 50 μm) and quantification of adipocyte size in H&E sections. (**H**) GTT and AUC_{GTT}. (**I**) ITT and AUC_{ITT}. AUC, area under glucose curve. Data are shown as mean ± SEM ($n = 6$ mice for each group or 3 independent experiments). ns, no significance; *$P < 0.05$, **$P < 0.01$.

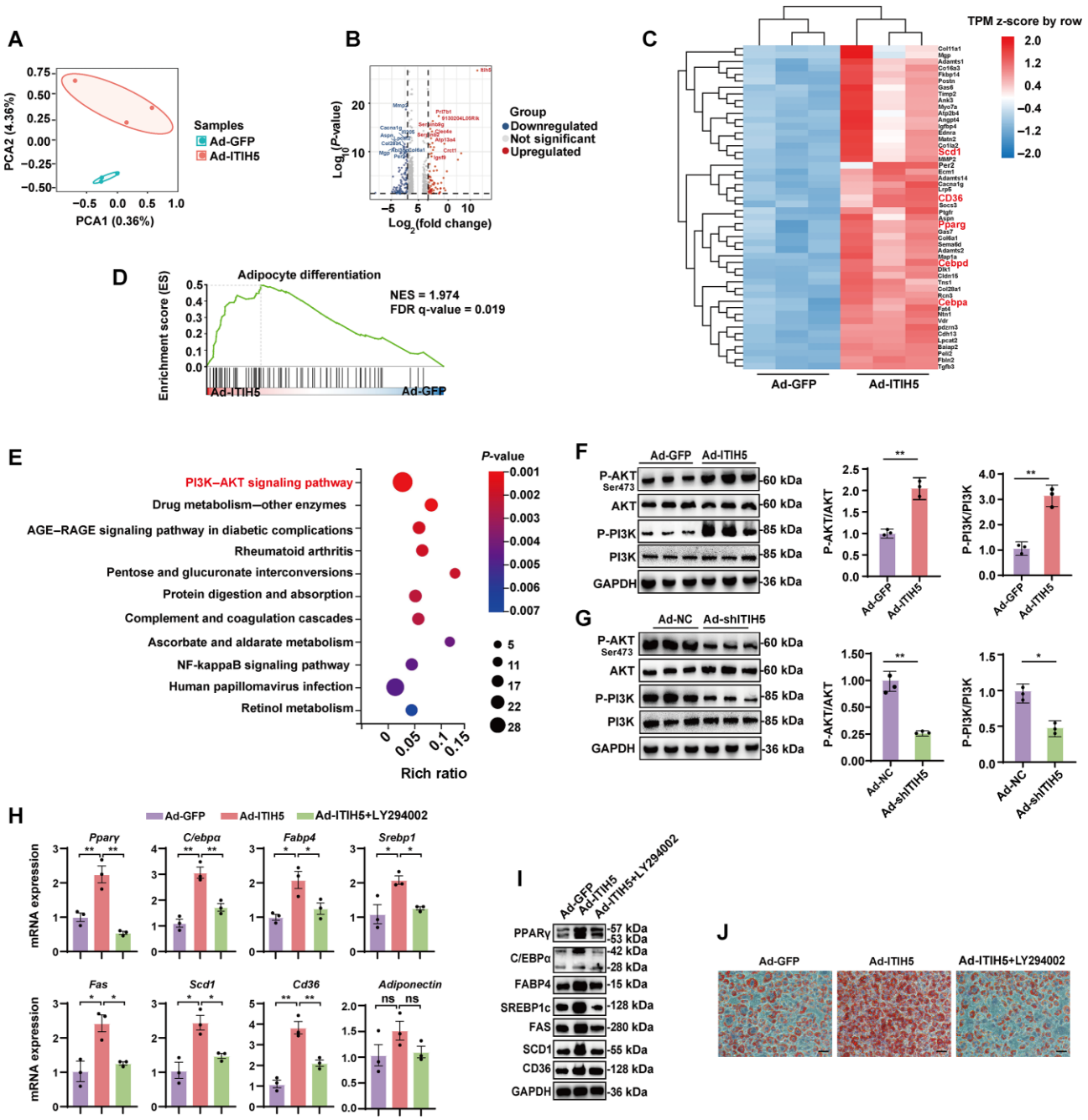


Figure 6 The regulation of adipogenesis by ITIH5 depends on the PI3K/AKT signaling pathway. (**A**) PCA score plot showing clear clusters in each group. (**B**) Volcano plot of RNA-seq analysis (fold change ≥ 1, $P < 0.05$). (**C**) Heatmap for genes associated with lipid metabolism. (**D**) GSEA enrichment analysis for adipogenesis-related genes. (**E**) KEGG enrichment analysis for metabolic signaling pathways. (**F**–**J**) SVFs from WT mice were induced to differentiate into mature MPA. The cells were either transfected with Ad-ITIH5 or Ad-GFP, with or without LY294002 (10 μM) for 30 min, or transfected with Ad-shITIH5 or Ad-NC as indicated. (**F** and **G**) AKT and PI3K phosphorylation levels. Total protein loading: 30 μg. (**H** and **I**) The mRNA and protein expression of genes related to adipogenesis. Total protein loading: 30 μg. (**J**) Oil-Red-O staining. Data are shown as mean ± SEM ($n \geq 3$ independent experiments). *$P < 0.05$, **$P < 0.01$.

The adipose tissue primarily consists of subcutaneous adipose tissue (e.g. iWAT) and visceral adipose tissue (e.g. eWAT). These two depots possess distinct biological properties that differentially affect local and systemic metabolic function (Karaskova et al., 2021; Lazarescu et al., 2025). Thus, gene functions can vary significantly across different adipose depots. However, it remains unclear whether ITIH5 expression is depot-specific. We found that ITIH5 was highly expressed

in both eWAT and iWAT. Here, we primarily investigated the metabolic role of ITIH5 in the iWAT. Further studies in other adipose tissues, particularly in the eWAT, will be important to fully establish the physiological relevance of ITIH5.

ECM remodeling is considered a key factor in determining the metabolic function of the adipose tissue (Sakers et al., 2022). Excess ECM deposition, i.e. fibrosis, restricts the expansion of adipocytes and promotes ectopic fat deposition, leading to insulin resistance and metabolic dysfunction (Yu et al., 2025). Conversely, ECM degradation promotes adipocyte plasticity and reshapes metabolic adaptability (Sakers et al., 2022; Auger and Kajimura, 2023; Yu et al., 2025). Previous studies showed that ITIH5 is a homeostatic regulator of ECM, maintaining matrix integrity by regulating ECM synthesis and degradation (Rose et al., 2017; Wu et al., 2025). In this study, we found that ITIH5 knockdown significantly downregulated Collagen I, Collagen III, and TIMP1 expression and upregulated MMP9 expression, whereas ITIH5 overexpression exhibited the opposite effects *in vitro*. In *in vivo* experiments, ITH5 knockdown also reduced ECM deposition in the iWAT of HFD-fed mice. These results confirmed the critical role of ITIH5 in ECM remodeling. Accumulating evidence suggests that ECM-secreted proteins are not only structural scaffolds of cells but also regulate cell behavior as signaling molecules by interacting with cell surface receptors, such as regulating adipocyte differentiation and function (Nie et al., 2008; Ding et al., 2024; Sleeboom et al., 2024). Our findings support the role of ITIH5 as an ECM-secreted protein (Wu et al., 2025), which may interact with cell surface receptors (e.g. integrins and CD44), activating the downstream PI3K–Akt signaling cascade (Martin et al., 2016; Kosinski et al., 2024; Wu et al., 2025), thereby regulating adipocyte differentiation and function (Feng et al., 2025). In addition, previous studies reported that PI3K/Akt can upregulate CD36 through SREBP1c-dependent mechanisms (Tian et al., 2026). Herein, we found that ITIH5 simultaneously regulated PI3K/AKT phosphorylation and CD36 expression, and the PI3K/AKT inhibitor LY294002 reversed these effects. These results indicate that ITIH5 at least partially upregulates CD36 through the PI3K/AKT pathway to promote fatty acid uptake and lipid accumulation.

Adipose tissue inflammation is a core driver of obesity-related insulin resistance (Bruder and Bruder-Nascimento, 2025; Lin and Jensen, 2025). In this study, we found that ITIH5 overexpression promoted AKT phosphorylation as well as the expression and secretion of IL-6. Consistent with previous reports (Sakers et al., 2022; Sutherland et al., 2023; Zheng et al., 2026), these results indicate that ITIH5 may regulate adipose tissue inflammation by modulating ECM remodeling and the PI3K/AKT pathway. The mechanism needs further investigation.

Notably, ITIH5 exhibits dual regulation of ECM homeostasis and adipose thermogenesis. We found that ITIH5 knockdown increased UCP1 and cAMP levels in mice, accompanied by elevated energy expenditure. These changes may be attributed to ECM remodeling, which alters the adipose tissue microenvironment and has been shown to promote WAT browning (Takata et al., 2020). In addition, previous studies showed that PI3K–Akt signaling regulates the expression of thermogenic genes, such as UCP1 (Wu et al., 2017; Song et al., 2018). Therefore, we propose that ITIH5 may affect WAT browning and thermogenesis through two distinct mechanisms: ECM remodeling and PI3K/AKT signaling.

Despite revealing the metabolic regulatory role of ITIH5, this study has several limitations. (i) The mechanistic exploration was insufficient. How does ITIH5 directly regulate the PI3K/AKT pathway? Does ITIH5 interact with the PI3K/AKT pathway through specific receptors or the ECM? Protein interaction screening is needed to clarify the upstream signaling mechanisms. (ii) Adipose depot specificity was not fully addressed. As the experiments focused solely on the iWAT, our ability to elucidate the potential functional differences of ITIH5 across distinct adipose depots was limited. Given the well-established metabolic differences between subcutaneous (e.g. iWAT) and visceral (e.g. eWAT) fat, further investigation into the role of ITIH5 in different adipose tissues is warranted. (iii) Clinical relevance was yet to be validated. For instance, the expression pattern of ITIH5 in human obese patients and its correlation with metabolic markers have not been assessed. Future research should explore the potential of ITIH5 as a therapeutic target for obesity, such as developing ITIH5 inhibitors specifically targeting the adipose tissue or investigating its interactions with known metabolic regulators (e.g. adiponectin andand leptin).

In conclusion, this study confirms that ITIH5 is a key regulator of adipocyte differentiation and the progression of obesity. It promotes lipid accumulation and inflammation through the activation of the PI3K/AKT pathway. These findings not only expand our understanding of the functional diversity of the ITIH protein family, but also provide new insights for the treatment of obesity and related metabolic diseases. Future research should further elucidate the molecular network of ITIH5 and explore its clinical translational potential.

Materials and methods

Experimental animals

The 8-week-old male C57BL/6 J (WT) mice, ob/ob mice, and db/db mice (GemPharmatech Co., Ltd) were housed in an environment with a temperature of 25°C, alternating light and dark for 12 h, and appropriate humidity. To establish a HFD-induced obesity model, WT mice were fed a HFD (60% fat, Catalog no. D12492) or a ND for 12 weeks. At the end of the experiment, the animals were euthanized, and tissue samples were frozen in liquid nitrogen for storage. This study was approved by the Animal Ethics Committee of Chongqing Medical University (IACUC-CQMU-2024-0479).

Cell culture and differentiation

3T3-L1 cells were cultured in Dulbecco's Modified Eagle Medium (DMEM) high-glucose medium (4.5 g/L D-glucose, Biological Industries) and maintained at 37°C with 5% CO_2. Once the cells reached 100% confluence after 2 days (Day 0), the medium was replaced with DMEM high-glucose medium containing 0.5 mM 3-isobutyl-1-methylxanthine (IBMX), 1 μM dexamethasone (Dex), 10 μg/ml insulin, and 10% fetal bovine serum (FBS) to induce differentiation. The cells were then maintained in DMEM high-glucose medium containing 10 μg/ml insulin for 48 h. On Day 4, medium was refreshed with DMEM high-glucose medium with 10% FBS. This medium was changed every 48 h until the cells were fully differentiated into mature adipocytes.

Isolation and differentiation of SVFs

SVFs were isolated from the iWAT of mice as previously described (Fang et al., 2024). Briefly, the adipose tissue was chopped and incubated with type I collagenase (1.5 g/L, Sigma) for 30 min. The digestion was inactivated with complete medium. Subsequently, the cell suspension was centrifuged, washed, and passed through a 40-μm filter. Then, the cells were inoculated in 10-cm dishes and induced to differentiate into mature adipocytes.

Adenovirus transfection

3T3-L1 cells or MPA were cultured in 10-cm dishes. When the cells reached 80% confluence, they were transfected with adenovirus for 48 h. The ITIH5-overexpressing adenovirus (Ad-CMV-ITIH5-EGFP, Ad-ITIH5) and its control (Ad-CMV-EGFP, Ad-GFP), as well as the ITIH5 knockdown adenoviruses (Ad-hU6-shRNA-ITIH5-EGFP, Ad-shITIH5-1, Ad-shITIH5-2, and Ad-shITIH5-3) and their control (Ad-hU6-shRNA-Scramble-EGFP, Ad-NC), were provided by Genechem Co., Ltd The sequences for shITIH5 were: 5′-ccTGAGGAATACGGCAAGAAT-3′ (shITIH5-1), 5′-gaATGGGATCTTGGGAGATTT-3′ (shITIH5-2), and 5′-ccTCAGACGATAATGAAGAAA-3′ (shITIH5-3). For *in vivo* experiments, 8-week-old male WT mice were fed a ND or a HFD for 12 weeks before virus injection. After successful modeling, ITIH5-overexpressing or knockdown adenoviruses (1×10^9 pfu/ml) were injected into the inguinal fat pads of mice, with five injection points (20 μl per point) per side (Zeng et al., 2025), once a week for three consecutive weeks. Throughout the experiment, body weight, food intake, and rectal temperature were monitored. At the end of the study, the mice were euthanized, and tissues were collected.

Oil-Red-O staining

As previously described (Zhang et al., 2019), on Days 3, 6, 9, and 12 after the initiation of differentiation, cells were washed three times with phosphate-buffered saline (PBS) and fixed with 10% formaldehyde for 30 min at 25°C. Then, the cells were stained with Oil-Red-O solution (0.3%, Sigma) for 1 h. To measure lipid content, the lipid droplets were solubilized with 100% isopropanol, and absorbance was recorded at 510 nm.

qRT-PCR and western blotting

qRT-PCR was performed as previously described. *Gapdh* was used as a control gene. The primer pairs were listed in Supplementary Table S1. Protein expression was analyzed by western blotting as described previously (Qiu et al., 2024). The primary antibodies used included anti-ITIH5 antibody (1:1000, Santa Cruz Biotechnology), anti-PPARγ antibody (1:1000, Cell Signaling Technology), anti-CEBPα antibody (1:1000, Cell Signaling Technology), anti-CD36 antibody (1:1000, Abcam), anti-FAS antibody (1:1000, Cell Signaling Technology), anti-SCD1 antibody (1:1000, Abcam), anti-FABP4 antibody (1:1000, Abcam), anti-SREBP1c antibody (1:1000, Abcam), anti-UCP1 antibody (1:5000, Abcam), anti-Collagen I antibody (1:1000, Proteintech), anti-Collagen III antibody (1:1000, Proteintech), anti-MMP9 antibody (1:1000, Proteintech), anti-TIMP1 antibody (1:1000, ZEN-BIOSCIENCE), anti-PI3K antibody (1:1000, Cell Signaling Technology), anti-Phospho-PI3K antibody (1:1000, Cell Signaling Technology), anti-AKT antibody (1:1000, Cell Signaling Technology), anti-Phospho-AKT antibody (1:1000, Cell Signaling Technology), and anti-GAPDH (1:1000, CUSABIO).

Histological analysis

The adipose tissue was fixed with 4% paraformaldehyde, embedded in paraffin, sectioned into 5-μm-thick sections, and processed for Sirius Red, Masson's trichrome, and hematoxylin and eosin (H&E) staining. The size of adipocytes in the iWAT was quantitatively analyzed using ImageJ software. IHC staining was performed in the iWAT following the standard protocol described previously (Qiu et al., 2024). The slides were blocked with 3% bovine serum albumin and then incubated with primary antibodies against F4/80 (anti-F4/80, 1:200, HUABIO) and ITIH5 (anti-ITIH5, 1:50, Santa Cruz Biotechnology) at 4°C overnight. Subsequently, biotinylated goat anti-rabbit immunoglobulin was applied on the section and incubated for 20 min at 37°C. Finally, the sections were visualized using diaminobenzidine.

GTT and ITT

For the GTT, mice were fasted for 16 h and given an intraperitoneal injection of glucose (1 g/kg body weight). For the ITT, mice were fasted for 6 h and injected with insulin (0.75 IU/kg body weight). Glucose levels in blood samples from the tail vein were monitored at various time points (0, 15, 30, 60, 90, and 120 min).

Metabolic phenotype analysis

Indirect calorimetry was performed by using an animal monitoring system (Clams; Oxymax) to measure VO_2, VCO_2, body weight, food intake, and energy expenditure. Metabolic

parameters were recorded for each mouse over two days, following a 24-h acclimation period. The average data from the second day were used for analysis.

ELISA

ITIH5 and IL-6 levels in cell culture supernatants from 3T3-L1 cells and MPA were measured using an ELISA kit (ELK Biotechnology). For cAMP measurement, the iWAT was homogenized in PBS containing protease inhibitors. After centrifugation, cAMP levels were evaluated using another ELISA kit (JONLNBIO) according to the manufacturer's instructions.

RNA-seq analysis

Total RNA was extracted using Trizol (Invitrogen) reagent with three replicate samples per group, and the extraction steps were performed according to the instructions. BGISEQ-500 sequencer was used for RNA-seq analysis (BGI-Shenzhen). All data were analyzed by the software Dr Tom (http://report.bgi.com) (You et al., 2022).

Statistical analysis

Statistical analysis was performed using Prism software version 10.0 (GraphPad), and the data are presented as mean ± SEM. ImageJ software was used to analyze cell size. A two-tailed unpaired Student's *t*-test was used for comparison between two groups, with $P < 0.05$ considered statistically significant.

Supplementary material

Supplementary material is available at *Journal of Molecular Cell Biology* online.

Acknowledgements

We appreciate the technical help from the College of Laboratory Medicine, Chongqing Medical University for performing experiments. Schematic diagrams were created with Biorender.com. We also thank Dr Xi Li (Biology Science Institutes, Chongqing Medical University) for providing the 3T3-L1 cell lines.

Funding

This study was supported by grants from the National Natural Science Foundation of China (82170816 and U22A20289).

Conflict of interest: none declared.

Author contributions: D.L.: methodology, formal analysis, data curation, investigation, and writing—original draft. M.X.: methodology, data curation, and investigation. J.L.: methodology, data curation, and investigation. M.Y.: conceptualization, writing—review and editing, and funding acquisition. G.Y.: conceptualization, writing—review and editing, and funding acquisition. L.L.: conceptualization, methodology, supervision, writing—review and editing, and funding acquisition. All authors read and approved the final manuscript.

References

Anveden, Å., Sjöholm, K., Jacobson, P., et al. (2012). ITIH-5 expression in human adipose tissue is increased in obesity. Obesity *20*, 708–714.

Auger, C., and Kajimura, S. (2023). Adipose tissue remodeling in pathophysiology. Annu. Rev. Pathol. *18*, 71–93.

Blüher, M. (2019). Obesity: global epidemiology and pathogenesis. Nat. Rev. Endocrinol. *15*, 288–298.

Bond, S.T., Calkin, A.C., and Drew, B.G. (2022). Adipose-derived extracellular vesicles: systemic messengers and metabolic regulators in health and disease. Front. Physiol. *13*, 837001.

Bruder, A., and Bruder-Nascimento, T. (2025). Adipose tissue-derived adipokines in vascular physiology and pathophysiology: insights and implications. Compr. Physiol. *15*, e70018.

Chan, P., Risler, J.L., Raguenez, G., et al. (1995). The three heavy-chain precursors for the inter-alpha-inhibitor family in mouse: new members of the multicopper oxidase protein group with differential transcription in liver and brain. Biochem. J. *306*, 505–512.

Chen, X., Rivard, L., Naqvi, S., et al. (2016). Expression and localization of inter-alpha inhibitors in rodent brain. Neuroscience *324*, 69–81.

Choi, J.W., Liu, H., Choi, D.K., et al. (2012). Profiling of gender-specific rat plasma proteins associated with susceptibility or resistance to diet-induced obesity. J. Proteomics *75*, 1386–1400.

Dai, Z.H., Wan, K.W., Wong, P.S., et al. (2025). Additional effect of exercise to intermittent fasting on body composition and cardiometabolic health in adults with overweight/obesity: a systematic review and meta-analysis. Curr. Obes. Rep. *14*, 54.

Desoye, G., and Hauguel-de Mouzon, S. (2007). The human placenta in gestational diabetes mellitus. The insulin and cytokine network. Diabetes Care *30*, S120–S126.

Ding, F., Zheng, P., Yan, X.Y., et al. (2024). Adipocyte-secreted PRELP promotes adipocyte differentiation and adipose tissue fibrosis by binding with $p75^{NTR}$ to activate FAK/MAPK signaling. Int. J. Biol. Macromol. *279*, 135376.

Fang, L., Liu, C., Jiang, Z.Z., et al. (2024). Annexin A1 binds PDZ and LIM domain 7 to inhibit adipogenesis and prevent obesity. Signal. Transduct. Target. Ther. *9*, 218.

Feng, Y., Zhang, H., Wu, W., et al. (2025). Roles of focal adhesion proteins in obesity related metabolic syndrome. Life Sci. *378*, 123808.

Gourgari, E., Ma, J., Playford, M.P., et al. (2019). Proteomic alterations of HDL in youth with type 1 diabetes and their associations with glycemic control: a case-control study. Cardiovasc. Diabetol. *18*, 43.

Hamm, A., Veeck, J., Bektas, N., et al. (2008). Frequent expression loss of Inter-alpha-trypsin inhibitor heavy chain (ITIH) genes in multiple human solid tumors: a systematic expression analysis. BMC Cancer *8*, 25.

Hutadilok, N., Ghosh, P., and Brooks, P.M. (1988). Binding of haptoglobin, inter-alpha-trypsin inhibitor, and alpha 1 proteinase inhibitor to synovial fluid hyaluronate and the influence of these proteins on its degradation by oxygen derived free radicals. Ann. Rheum. Dis. *47*, 377–385.

Karaskova, E., Velganova-Veghova, M., Geryk, M., et al. (2021). Role of adipose tissue in inflammatory bowel disease. Int. J. Mol. Sci. *22*, 4226

Khaliq, S.A., Park, S.Y., Maham, S., et al. (2025). ARHGEF3 coordinates adipocyte hypertrophy and differentiation through dual YAP–RhoA and PPARγ activation. J. Adv. Res. *79*, 445–460.

Kim, T.H., Koo, J.H., Heo, M.J., et al. (2019). Overproduction of inter-α-trypsin inhibitor heavy chain 1 after loss of $G\alpha_{13}$ in liver exacerbates systemic insulin resistance in mice. Sci. Transl. Med. *11*, eaan4735

Kosinski, J., Sechi, A., Hain, J., et al. (2024). ITIH5 as a multifaceted player in pancreatic cancer suppression, impairing tyrosine kinase signaling, cell adhesion and migration. Mol. Oncol. *18*, 1486–1509.

Lazarescu, O., Ziv-Agam, M., Haim, Y., et al. (2025). Human subcutaneous and visceral adipocyte atlases uncover classical and nonclassical adipocytes and depot-specific patterns. Nat. Genet. *57*, 413–426.

Li, T., Liu, Y., Cao, J., et al. (2025). Triphenyl phosphate induces lipid metabolism disorder and promotes obesity through PI3K/AKT signaling pathway. Environ. Int. *198*, 109428.

Lin, S., and Jensen, M.D. (2025). Human adipose tissue metabolism in obesity. J. Obes. Metab. Syndr. *34*, 105–119.

Liu, W., Yu, L., Chen, Q., et al. (2025). Poria cocos polysaccharides alleviate obesity-related adipose tissue insulin resistance via gut microbiota-derived short-chain fatty acids activation of FGF21/PI3K/AKT signaling. Food Res. Int. *215*, 116671.

Martin, J., Midgley, A., Meran, S., et al. (2016). Tumor necrosis factor-stimulated gene 6 (TSG-6)-mediated interactions with the inter-α-inhibitor heavy Chain 5 facilitate Tumor growth factor β1 (TGFβ1)-dependent fibroblast to myofibroblast differentiation. J. Biol. Chem. *291*, 13789–13801.

Nie, J., Chang, B., Traktuev, D.O., et al. (2008). IFATS collection: combinatorial peptides identify α5β1 integrin as a receptor for the matricellular protein SPARC on adipose stromal cells. Stem Cells *26*, 2735–2745.

Qiu, S., Wu, Q., Wang, H., et al. (2024). AZGP1 in POMC neurons modulates energy homeostasis and metabolism through leptin-mediated STAT3 phosphorylation. Nat. Commun. *15*, 3377.

Rose, M., Kloten, V., Noetzel, E., et al. (2017). ITIH5 mediates epigenetic reprogramming of breast cancer cells. Mol. Cancer *16*, 44.

Sakers, A., De Siqueira, M.K., Seale, P., et al. (2022). Adipose-tissue plasticity in health and disease. Cell *185*, 419–446.

Santoro, A., and Kahn, B.B. (2023). Adipocyte regulation of insulin sensitivity and the risk of type 2 diabetes. N. Engl. J. Med. *388*, 2071–2085.

Sleeboom, J.J.F., van Tienderen, G.S., Schenke-Layland, K., et al. (2024). The extracellular matrix as hallmark of cancer and metastasis: from biomechanics to therapeutic targets. Sci. Transl. Med. *16*, eadg3840.

Song, N.J., Chang, S.H., Kim, S., et al. (2018). PI3Kα–Akt1-mediated Prdm4 induction in adipose tissue increases energy expenditure, inhibits weight gain, and improves insulin resistance in diet-induced obese mice. Cell Death. Dis. *9*, 876.

Sutherland, T.E., Dyer, D.P., and Allen, J.E. (2023). The extracellular matrix and the immune system: a mutually dependent relationship. Science *379*, eabp8964.

Takata, K., Goto, T., Kuroda, M., et al. (2020). Stiffness of the extracellular matrix regulates differentiation into beige adipocytes. Biochem. Biophys. Res. Commun. *532*, 205–210.

Tian, M., Zhang, B., Li, H., et al. (2026). Oleic acid promotes milk fat synthesis by stimulating GPR40–$G\alpha_q$–PI3K/Akt–SREBP1-dependent fatty acid uptake. J. Agric. Food Chem. *74*, 6767–6779.

Tvarijonaviciute, A., Ceron, J.J., de Torre, C., et al. (2016). Obese dogs with and without obesity-related metabolic dysfunction—a proteomic approach. BMC Vet. Res. *12*, 211.

Wang, X., Huang, M., Lu, Y., et al. (2025). Integrated metabolomics and network pharmacology reveal the PI3K/Akt-mediated therapeutic mechanism of Abrus cantoniensis in lipid metabolism disorders. Phytomedicine *145*, 156953.

Wu, R., Liu, X.M., Sun, J.G., et al. (2017). DJ-1 maintains energy and glucose homeostasis by regulating the function of brown adipose tissue. Cell Discov. *3*, 16054.

Wu, Y., Meng, L., Zhan, S., et al. (2025). ITIH5-mediated fibroblast/macrophage crosstalk exacerbates cardiac remodelling after myocardial infarction. J. Transl. Med. *23*, 224.

You, M., Liu, Y., Wang, B., et al. (2022). Asprosin induces vascular endothelial-to-mesenchymal transition in diabetic lower extremity peripheral artery disease. Cardiovasc. Diabetol. *21*, 25.

Yu, H., Yang, F., Yan, D., et al. (2025). Fibulin-7 in progenitor cells promotes adipose tissue fibrosis and disrupts metabolic homeostasis in obesity. Protein Cell *17*, 212–230.

Zeng, T., Xiao, L., Li, J., et al. (2025). Adipocyte RNA-binding protein CELF1 promotes beiging of white fat through stabilizing Dio2 mRNA. Nat. Commun. *16*, 7414.

Zhang, C., Luo, X., Chen, J., et al. (2019). Osteoprotegerin promotes liver steatosis by targeting the ERK–PPAR-γ–CD36 pathway. Diabetes *68*, 1902–1914.

Zheng, H., Tang, D., An, S., et al. (2026). Allicin protects against inflammation via suppression of PI3K/AKT/NF-κB signaling pathway in the model of acute cutaneous injury mouse and LPS-induced keratinocyte. Int. Immunopharmacol. *174*, 116331.

Zhuo, L., Hascall, V.C., and Kimata, K. (2004). Inter-alpha-trypsin inhibitor, a covalent protein–glycosaminoglycan–protein complex. J. Biol. Chem. *279*, 38079–38082.

Received November 23, 2025. Revised February 27, 2026. Accepted March 15, 2026.

© The Author(s) (2026). Published by Oxford University Press on behalf of *Journal of Molecular Cell Biology*, CEMCS, CAS.
This is an Open Access article distributed under the terms of the Creative Commons Attribution-NonCommercial License (https://creativecommons.org/licenses/by-nc/4.0/), which permits non-commercial re-use, distribution, and reproduction in any medium, provided the original work is properly cited. For commercial re-use, please contact reprints@oup.com for reprints and translation rights for reprints. All other permissions can be obtained through our RightsLink service via the Permissions link on the article page on our site-for further information please contact journals.permissions@oup.com